Power Consumption Characteristics of an In-Line Silverson High Shear Mixer

M. Cooke, and T. L. Rodgers
School of Chemical Engineering & Analytical Science, The University of Manchester, Manchester M13 9PL, U.K

A. J. Kowalski
Unilever R&D, Port Sunlight Laboratory, Quarry Road East, Bebington, Wirral CH63 3JW, U.K

DOI 10.1002/aic.12703
Published online in Wiley Online Library (wileyonlinelibrary.com).

In-line rotor stator mixers differ from in-tank versions because the flow is often controlled independently of the rotor speed. For in-tank devices the turbulent power can be adequately described by single impeller type power number. For an in-line rotor-stator mixer it is found that the power transmitted by the rotor consists of a power term and a flow term. The constants in this expression are normally obtained from a multilinear regression of a large matrix of experiments. Two simplified methods of obtaining these constants from limited data sets by (1) torque measurement and (2) by heat balance are described herein. These are used to determine the constants for a Silverson 150/250 MS inline mixer with different rotor stator arrangements from the laminar to turbulent regimes. The power and Metzner-Otto constants determined are shown to be in good agreement to data for a larger matrix of experimental data. © 2011 American Institute of Chemical Engineers AIChE J, 00: 000–000, 2011

Keywords: in-line rotor-stator mixers, Newtonian, non-Newtonian, power number, shear rate

Introduction

High shear rotor-stator mixers are widely used in process industries including the manufacture of many food, cosmetic, health care products, fine chemicals and pharmaceuticals. Rotor-stator devices provide a focussed delivery of energy, power and shear to accelerate physical processes such as mixing, dissolution, emulsification and deagglomeration.[1] To reliably scale-up these devices we need to understand the relationship between rotor speed, flow rate and the energy dissipated by these devices. The first step in reliable scale-up is to link the energy dissipation rate to desired process results and in turn to:

- process variables (rotor speed & flow rate), and
- design (size and geometry).

Then we can move on to understanding the important process operations listed earlier.

Atiemo-Obeng and Calabrese (2004)[2] state that:

- "The current understanding of rotor-stator devices has almost no fundamental basis.
- There are few theories by which to predict, or systematic experimental protocols by which to assess, the performance of these mixers.
- In fact there are few archival publications on rotor-stator processing".

Turbulent power for a batch rotor stator device can be described by a single "tank" type impeller power number, Po, Eq. 1,[2–4] where D is the impeller diameter and P is the shaft power for the impeller.

$$\mathrm{Po} = \frac{P}{\rho N^3 D^5} \tag{1}$$

The Po is essentially constant at Reynolds numbers greater than 10^4 in a baffled stirred vessel.[5] For rotor stator devices, previous studies[3,4] highlighted some uncertainty as to whether the regime was in the laminar or turbulent region. This regime is governed by the mixing Reynolds number, Re, Eq. 2, where h is a characteristic length, ρ is the liquid density, N is the impellor speed, and μ is the viscosity.

$$\mathrm{Re} = \frac{\rho N D h}{\mu} \tag{2}$$

For the Silverson, there are several ways of calculating what the Reynolds number is, depending on how h is defined, either as the impeller diameter, D, or as the screen hole diameter, d_h, or as the rotor-stator gap, $D_{s,o} - D_{r,o}$ or $D_{s,i} - D_{r,i}$. The regime will change from laminar to fully turbulent depending on the definition of h used. In the previous studies mentioned[3,4] it was assumed the characteristic length used should be the swept impeller diameter, giving Eq. 3 (the same as for a stirred tank)—an assumption which was felt to be justified in the face of the good quality of predictions subsequently obtained.

$$\mathrm{Re} = \frac{\rho N D^2}{\mu} \tag{3}$$

For an in-line rotor-stator mixer the flow through the rotor can be controlled independently of the rotor speed (unlike in a

Correspondence concerning this article should be addressed to M. Cooke at michael.cooke@manchester.ac.uk.

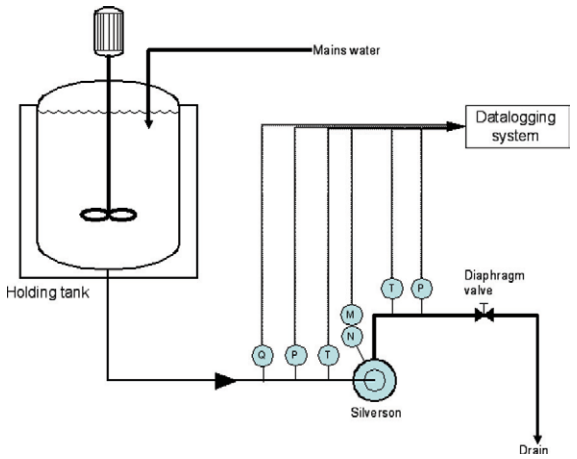

Figure 1. Schematic of experimental rig.

[Color figure can be viewed in the online issue, which is available at wileyonlinelibrary.com.]

stirred tank) or can be a function of material properties since, even when the flow rate in the mixer head is fully turbulent, the inlet and outlet flow often is not turbulent, especially for shear thinning materials. It has been found experimentally that the power number for in-line devices is dependent on the flow.[1,6,7–9] As the power depends on flow rate a single power number is not adequate. Kowalski (2009)[6] showed that the total rotor power can be assumed to be the sum of three powers as, in Eq. 4:

$$P = P_T + P_F + P_L \tag{4}$$

The first term on the right of Eq. 4, P_T, reflects the typical power used in a stirred vessel and if the regime is turbulent (Re $\geq 10^4$) then the Po is independent of the Reynolds number, Re, and Eq. 1 is used with a constant power number based on zero flow, Po_Z.

The second term on the right hand side of Eq. 4, P_F, reflects the power drawn due to the flow of fluid through the chamber which is then convected away from the device. It may be defined[6] as Eq. 5, where Q_M is the mass flow rate.

$$P_F = k_1 Q_M N^2 D^2 \tag{5}$$

Combining Eqs. 1 and 5 with Eq. 4 produces Eq. 6 which is the expression proposed by Kowalski (2009)[6] for power draw of an in line rotor-stator mixer in the turbulent regime.

$$P = Po_Z \rho N^3 D^5 + k_1 Q_M N^2 D^2 + P_L \tag{6}$$

The term P_L accounts for losses which, for the inline rotor stator, are mainly losses in the bearings. These may not be constant (vary with speed) so need to be separately measured and accounted for.

If however the regime is laminar, then there is a dependency of Po_Z on Re which is described by Eq. 7,[5] where k_0 is a constant. This term is similar to that used in conventional stirred tank analysis and in keeping with this usage the distinction between laminar and turbulent regimes is made.

$$Po_Z \, Re = k_0 \tag{7}$$

Substituting the Reynolds number from Eq. 3 and the power number from Eq. 1 in Eq. 7 produces a term for the power required to rotate the shaft in response to the resistance of the liquid in the process chamber in the laminar regime, P_I, Eq. 8.

$$P_T = k_0 N^2 D^3 \mu \tag{8}$$

Substituting Eq. 8 into Eq. 4 instead of Eq. 1 now produces an analogous equation to Eq. 6 but for the laminar regime, Eq. 9

$$P = k_0 N^2 D^3 \mu + k_1 Q_M N^2 D^2 + P_L \tag{9}$$

The values of the constants are fitted from the collected data.

Experimental Equipment and Materials and Methods

Experimental equipment

Figure 1 is a schematic of the experimental rig used for these experiments. This consists of a specially commissioned high speed 150/250 MS Silverson in-line rotor stator mixer. The 150/250 notation indicates the swept diameter of the rotor, 1.5 inches for the inner rotor and 2.5 inches for the outer rotor. All the power calculations in this article are based on the designated outer swept diameter, D, of 2.5 inches (0.0635 m). It is normally fitted with standard double emulsifier screen (Figure 2). This rotor was also run with a fine emulsifier stator (Figure 3) and with the stator removed. Details of the rotor stators are provided in Table 1. The clearance between rotors and stators, e.g., $D_{s,o} - D$, are nominally 9 thousandth of an inch (0.2286×10^{-3} m) and the stator thicknesses are 0.072 inches (1.83×10^{-3} m). See Figure 3 for details of the nomenclature used for the stator dimensions.

For turbulent power measurements, the Silverson is gravity fed with water at constant head and ambient temperature from a 1 m^3 vessel. The water flow rate is controlled using a valve downstream of the Silverson and the flow rate is measured using a MICRO MOTION COLIOLIS R-SERIES mass flow meter. The Silverson is skid mounted and equipped with PT100 temperature probes to measure the inlet and outlet temperature, T. The rotor speed range is 0 to 12,000 rpm, controlled by an inverter over the range 0–200 Hz. An oversized motor 22 kW is used to provide adequate power and torque up to the maximum speed and the drive shaft is segmented to include an in-line torque sensor. The shaft torque, M, and the speed, N, are measured on the drive shaft using a 20 Nm RWT 321 Transducer supplied by Sensor Technology (Figure 4). Inlet and outlet pressures, p, are measured using pressure transducers. All instrument data are logged and controlled on an EMERSONS DeltaV data logging and

Figure 2. Standard double emulsification screen setup (a) the rotor (b) the screens.

[Color figure can be viewed in the online issue, which is available at wileyonlinelibrary.com.]

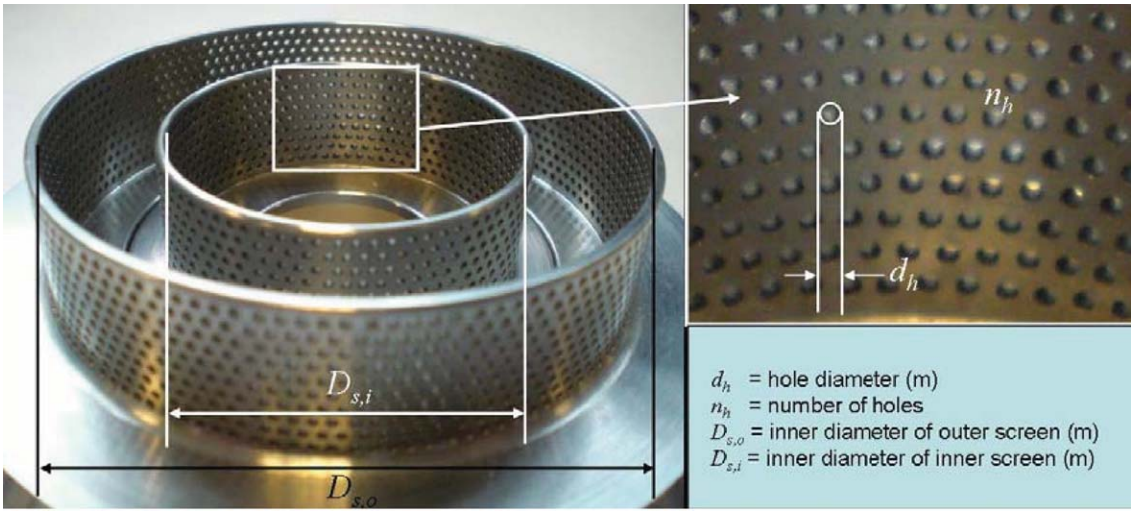

Figure 3. Screen dimension nomenclature (double screen fine emulsifier shown).

[Color figure can be viewed in the online issue, which is available at wileyonlinelibrary.com.]

control system. These data are saved and can be exported to a Microsoft Excel spreadsheet for analysis.

Solutions other than water were not sent to drain as indicated in Figure 1 but instead were fed on recycle loop from and returning to a 60 L batch mixer. The stainless steel jacketed vessel was temperature controlled and was normally fed by a tri-lobe pump. For experiments at free flow using the Silverson as the sole pump, the tri-lobe pump was bypassed once flow was established.

Materials and methods

Fluids and Rheology. Water, Silicon oil (polydimethylsiloxane, Dow Corning 200 fluid), and an aqueous solution of carboxymethyl cellulose (CMC), HERCULES POWDER grade 7H4C, were chosen as Newtonian and non-Newtonian fluids, respectively. The silicon oil used was either used as supplied or blended to obtain a wide range of viscosities. The viscosity range of the oil supplied was 10 to 10,000 centistokes (cSt). The rheological properties of the solutions were determined at a range of temperatures with a viscometer (Haake RV 20) by using the standard cup and bob Couette configuration using either the MV1 or MV2 bob dependant upon the viscosity range.

The viscosity of the silicon oils are sensitive to temperature changes, therefore the viscosity variation was measured between 15 and 50°C and found to fit to Eq. 10, where T is the absolute temperature and a and b are fitted constants given by Table 2. The viscosity of the Newtonian fluids ranged from 0.001 to 10 Pa s. Note that some of these solutions were blends and the designation is only approximate.

$$\mu = \frac{a}{T} + b \tag{10}$$

The rheological parameters of the non-Newtonian fluids were found to obey a power law, Eq. 11, where μ_a is the apparent viscosity, K is the consistency index, $\dot{\gamma}$ the average shear rate and n the flow behavior index.

$$\mu_a = K\dot{\gamma}^{n-1} \tag{11}$$

The viscosities of these fluids were also measured over a temperature range, 20 to 35°C. Both K and n were found to vary with temperature. However, as only a small dependency of the flow behavior index on temperature was found, this was averaged out and the resulting recalculated consistency indices were found to fit well to Eq. 12 with parameters given by Table 3.

$$\mu_a = \left(\frac{a}{T} + b\right)\dot{\gamma}^{n-1} \tag{12}$$

Power Measurement. Two methods of measuring power were used, by torque and by heat balance.

Torque. This was measured by an in-line torque meter fitted to the drive shaft. There are two main sources of potential error when measuring the torque on the rotor shaft. Firstly, the torque sensor used was found to exhibit a slight zero drift when operating the Silverson continuously over a number of hours. Secondly the sensor also measures bending moments on the shaft; this measurement cancels out over the course of 1 revolution of the shaft and so does not affect average shaft torque, but does make a static zero adjustment difficult.

To minimize these sources of error, the zero is measured before and after each run and the resulting values averaged.

Table 1. Size of the Double Rotor and Stator Configuration

	Standard Screen Dual Emulsifier		Fine Screen Dual Emulsifier	
Property	Inner, *i*	Outer, *o*	Inner, *i*	Outer, *o*
Screen hole diameter, d_h	1.588×10^{-3} m	1.588×10^{-3} m	0.794×10^{-3} m	0.794×10^{-3} m
Number of holes, n_h	300	560	675	1250
Number of rows n_r	6	7	9	10
Rotor diameter, D	0.0381 m	0.0635 m	0.0381 m	0.0635 m

Figure 4. TORQSENSE torque meter fitted to Silverson drive shaft.

[Color figure can be viewed in the online issue, which is available at wileyonlinelibrary.com.]

For the turbulent power, bending moments were eliminated by taking the zero value at 50 rpm with the outlet closed. The actual power drawn by the rotor at these conditions is negligibly low but bending moments are cancelled out by the averaging. The averaged "running" zero is subtracted from the measured value to give the shaft torque M.

For the laminar power the above method is not possible as the power number is inversely proportional to the Re and hence the torque at 50 rpm can be considerable. In this case a "real" zero is taken in three blocks with the rotor rotated between each at 50 rpm to spin the shaft to a different position between each zero measurement. Again this is done before and after each set of readings under conditions of zero flow-through. The mean of these values is subtracted from the operating torque to give the running torque value at the operating speed, N, which is averaged over the time at the equilibrium condition. Power measurements in the transitional regime were also taken by this method. The operating power, P, from torque is then calculated from Eq. 13.

$$P = 2\pi NM \tag{13}$$

Power from calorimetry (heat balance). Power measurement is also obtained by Calorimetry using the temperature rise of the fluid passing through the Silverson, Eq. 14, where Q_M is the mass flow rate, C_p is the specific heat, which for water is 4.192 J kg^{-1} K^{-1} at 10 °C and ΔT is the temperature rise through the Silverson.

Table 2. Values of Constants *a* and *b* used to Correct Newtonian Viscosities for Temperature, Eq. 10

Solution	*a*	*b*
10,000 cSt silicon oil	13,701	−36.47
2000 cSt silicon oil	2398	−6.32
1000 cSt silicon oil	1688	−4.62
800 cSt silicon oil	1013	−2.75
350 cSt silicon oil	618	−1.71
100 cSt silicon oil	141	−0.37
50 cSt silicon oil	54	−0.14
25 cSt silicon oil	24.3	−0.06
Water	1.705	−0.0048

Table 3. Values of the Constants for Eq. 12 for the Viscosities of the Non-Newtonian Fluids

Solution	*a*	*b*	*n*
2.5% CMC	87014.6	−200.6	0.218
2.25% CMC	78103.9	−196.1	0.233
2% CMC	64020.1	−153.9	0.240
1.25% CMC	19056.7	−49.9	0.342

$$P = Q_M C_p \Delta T \tag{14}$$

Measurements were generally made over a period of several minutes allowing 2 minutes to reach equilibrium and around 5 minutes averaging at equilibrium conditions. The data were inspected and data not at an equilibrium ΔT was not used in the power analysis.

Losses and Corrections. These shaft powers by heat and torque also contain losses in the shaft bearings. These bearing losses were also measured using the same methods (including the bearing losses associated with a 50 rpm running zero) with the shaft rotated at different speeds without the rotor attached. A spacer washer was used in place of the rotor to ensure the bearing was under the same tension. These data yield values of the lost power, P_L, which are subtracted from the measured power at the same conditions.

For temperature correction of the viscosity it was normal to use the outlet temperature. However, in the case of zero or low flow rates this temperature is not representative of the head temperature. Therefore a third PT100 temperature probe was inserted in the outer impeller port, flush to the inner wall, and this temperature was used for these cases. All the PT100s were calibrated against each other in situ by gravity feeding water through the Silverson to drain over a time period of one hour minimum with the Silverson switched off. The differences were low (<0.1°C). Any differences were corrected for in the calculations. The Silverson and the line work up to and including the temperature probes were well lagged to minimize losses.

Determination of the Turbulent Power Constants. The turbulent constants in the power equation can be fitted by applying multilinear regression analysis to fit data to Eq. 6. Cooke et al. (2008)[1] found that good estimates of the constants can be obtained using a simplified set of trials.

In Method 1 (which requires a torque meter) we note that there are two sets of conditions under which constant turbulent power numbers are obtained as follows.

With the losses accounted in Eq. 6 by measuring and subtracting bearing losses we produce Eq. 15.

$$P = \mathrm{Po_Z}\rho N^3 D^5 + k_1 Q_M N^2 D^2 \tag{15}$$

When the outlet valve is closed, so we have zero flow ($Q_M = 0$), then the power is a minimum given by Eq. 16.

$$P = \mathrm{Po_Z}\rho N^3 D^5 \tag{16}$$

When the valve is fully open and the rotor-stator device acts as the sole pumping agent then the flow rate Q_M is proportional to the rotor speed as Eq. 17, where N_Q is the flow rate constant or pumping number.

$$Q_M = \rho N_Q N D^3 \tag{17}$$

Figure 5 shows data for three different screen arrangements. From the gradients of these lines N_Q can be evaluated using

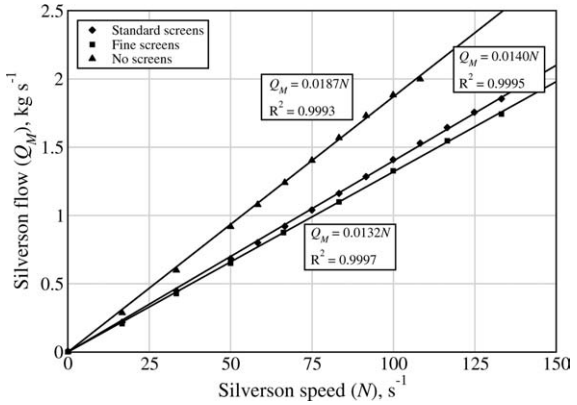

Figure 5. Silverson 150/250 MS with the dual rotor showing unfettered flow for three different stator screen arrangements—The standard dual emulsifier mesh; the fine emulsifier mesh and with no screens.

From Eq. 17 the gradient in each case = $N_Q\rho D^3$, hence N_Q can be evaluated.

Eq. 17 and these were found to vary from 0.051 with fine mesh screen to 0.072 when the screens are removed. These flow rate constants are an order of magnitude lower than those of a turbine in a stirred vessel, due to the flow constrictions imposed by the in-line geometry.

Power draw is a maximum given by $P_{max} = Po_U\rho N^3D^5$ which can also be expressed as $Po_Z\rho N^3D^5 + (Po_U - Po_Z)\rho N^3D^5$ with the characteristic power number Po_U. Substituting for Q_M in Eq. 15 and rearranging gives Eq. 18, which in turn yields Eq. 19.

$$P_{max} = (Po_Z + k_1N_Q)\rho N^3D^5 = Po_U\rho N^3D^5 \quad (18)$$

$$k_1 = \frac{Po_U - Po_Z}{N_Q} \quad (19)$$

In Method 2 we consider the example of a fixed speed device where flow rate can be varied by means of a backpressure valve. In this case the power is a linear function of the flow rate (Figure 7) where the intercept is given by $Po_Z\rho N^3D^5$ and the gradient by $k_1N^2D^2$ and thus Po_Z and k_1 can be determined.

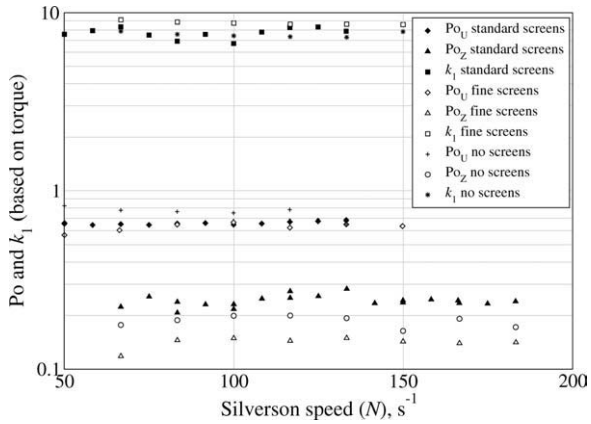

Figure 6. Silverson 150/250 MS fitted with the dual rotor.

Po_U, Po_Z, and k_1 values determined by Method 1 for fine and standard emulsifier screens compared with the values when no screens are fitted.

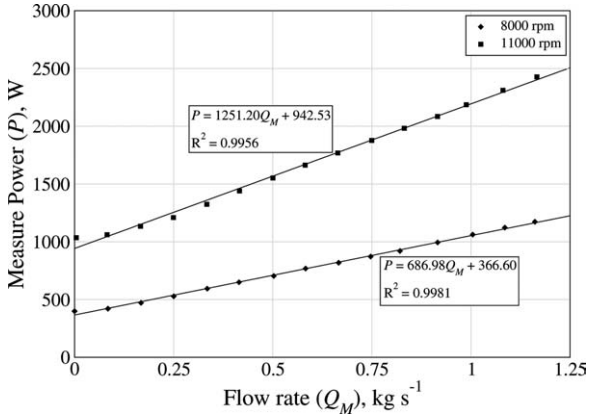

Figure 7. Evaluation of Silverson 150/250 MS flow constants graphically using Method 2.

Gradient = $k_1N^2D^2$ and intercept = $Po_Z\rho N^3D^5$, hence k_1 and Po_Z can be determined.

This method also has the advantage of being suitable with power measurement by heat balance.

Results and Discussions

Turbulent power results

Figure 6 presents examples of the values of Po_Z, Po_U, and k_1 determined by Method 1 for the Silverson 150/250 MS fitted with the dual rotor. It compares the fine and standard emulsifier screens with the values when no screens are fitted. These plots illustrate that for a given rotor-stator arrangement, the values are essentially constant for all rotor speeds.

Figure 7 is an example of a Method 2, graphical determination of these same constants determined for the dual rotor fitted with the fine emulsifier screen at two speeds. Po_Z and k_1 can be calculated directly from the linear regression of a straight line fits. These values may also be fitted from a multilinear regression of the power data fitted to Eq. 15 using for example the ANOVA regression program provided in Microsoft Excel. The ANOVA output contains all the statistics necessary to judge the quality of the fit. Knowing k_1 and Po_Z then with a N_Q value determined using Eq. 17, Po_U can be determined from Eq. 19.

It is noted from Figure 7 that at very low flows there is a deviation from the line with an unexpected increase in power not predicted by Eq. 15. This increase in power is even more pronounced in the case of the standard emulsifier screens.[9] It is too consistent to be dismissed as experimental error. Cooke and Kowalski (2009)[9] showed that this can be accounted for mathematically by use of a pump efficiency term. This increase in power is probably due to recirculation. With the down stream valve closed or heavily gagged then as the rotor blade approaches a hole, material is forced through. As the blade passes it sucks material back into the low pressure area behind the blades resulting in internal recirculation which from Eq. 15 increases the power draw. With the very small holes present in the fine mesh screen, this effect is reduced. The recirculation around the holes, along with the periodic nature of the flow has been measured and predicted for example by Utomo et al. (2008).[10]

An outcome of this increase in power at low flows is a small discrepancy in the prediction of power at low flow rates. Also values of power calculated from Calorimetry are not determined at zero flow and hence tend to yield a

Table 4. Values of the Constants for Turbulent for the Silverson 150/250 MS Inline Mixer with Different Stator Screen Arrangements

Stator type	Silverson speed (rpm)	Method	N_Q	Po_Z	Po_U	k_1
Fine holes	3000–8000	1	0.051	0.145	0.63	8.79
	8000	2		0.150	0.64	9.60
	11,000	2		0.149	0.62	9.24
	ALL	Regression		0.148	0.63	9.36
	Mean			*0.148*	*0.63*	*9.25*
	Std %			*0.002*	*0.008*	*0.340*
	Std			*1.68*	*1.35*	*3.67*
Standard holes	3000–7000	1	0.054	0.241	0.66	7.75
	6000	2		0.250	0.68	8.03
	11000	2		0.219	0.67	8.34
	ALL	Regression		0.231	0.66	7.95
	Mean			*0.235*	*0.67*	*8.02*
	Std %			*0.014*	*0.011*	*0.245*
	Std			*5.75*	*1.68*	*3.06*
No screens	3000–6000	1	0.072	0.203	0.70	6.93
	ALL	Regression		0.22	0.74	7.16
	Mean			*0.212*	*0.72*	*7.05*
	Std %			*0.012*	*0.023*	*0.160*
	Std			*5.62*	*3.26*	*2.27*

slightly lower estimate of Po_Z. As we are not generally concerned with very low flows these discrepancies are trivial.

Cooke et al. (2008)[1] recently described comparative data for Power predictions using heat balance vs. torque using the Methods 1 and 2 described herein. This work compared the errors inherent in both temperature and torque measurement. It is noted that for torque, increasing flow increases both torque and power and hence reduces error. For temperature increasing flow increases power but still decreases ΔT due to the higher flow so that for very high flows the ΔT can be very low increasing the errors. For low flows ΔT is high but torque is low.

Power measurements by torque on this equipment are generally slightly higher than by heat, on average by about 10%. This is quite a reasonable agreement. The torque transducer is regularly recalibrated and is considered the more accurate measurement. The slightly lower values for heat is almost certainly due to unaccounted heat losses which must occur even for a well lagged system.

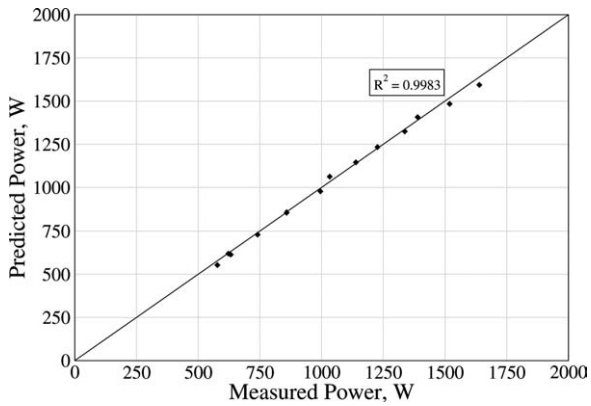

Figure 8. Compares the full flow measured power for the dual rotor fitted with the standard hole emulsifier screen with the line predicted from a multilinear regression fit to a large matrix of experiments on the same set-up.

Table 4 compares Method 1, Method 2 and multilinear regression turbulent power constants for the three stator arrangements considered. The agreements are very reasonable, generally within ±5% standard deviations which are considered to be within the measurement accuracy.

Figure 8 compares the full flow measured power for the dual rotor fitted with the standard emulsifier screen with the line predicted from a multilinear regression fit to a large matrix of experiments on the same set-up. This indicates that the constants derived from the short method give a good estimate of the power draw.

Full power draw analysis

The power consumption of an impeller with Newtonian fluids is usually expressed in the form of the dimensionless power number, Po, as a function of the Reynolds number, Re, where $Po = P/\rho N^3 D^5$ and $Re = \rho N D^2/\mu$. This procedure provides a characteristic power curve that depends only on impeller geometry and can be used to predict power requirements for any given fluid properties, impeller dimensions, and rotational speed. In the laminar regime, it is usual to determine the power constant $k_0 = PoRe$. For a Newtonian fluid, k_0 is a function of only the impeller geometry. This procedure would be expected to give a good fit to all free flow data. The original free flow data for all Newtonian fluids used is shown in Figure 9. This does not look like the characteristic power curve; instead it is a series of curves with the data for successive increasing viscosity moving to the left. The shape of this curve prompted a revisit to the error analysis.

As a result of this the losses in the bearings were measured. These measurements highlighted some interesting trends. When a ''true'' zero was used the torque loss was quite substantial. It was virtually constant (around 0.4 Nm) up to a speed of 8000 rpm giving a power loss proportional

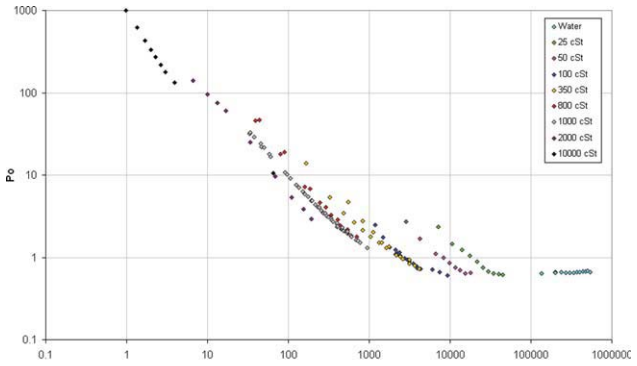

Figure 9. Power curve for Silverson 150/250 MS fitted with dual standard emulsifier rotor and stator.

Power numbers are NOT corrected for bearing losses. [Color figure can be viewed in the online issue, which is available at wileyonlinelibrary.com.]

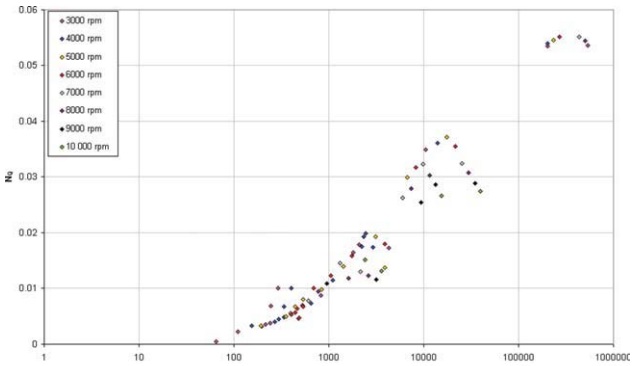

Figure 11. The effect of Re on the flow number for the standard dual rotor-stator.

[Color figure can be viewed in the online issue, which is available at wileyonlinelibrary.com.]

to N. Above 8000 rpm the torque loss increased with increasing speed giving a power loss proportional to around N^2.

A consequence of this is that for the fully turbulent (water) power data collected with a running zero of 50 rpm the correction was small and had very little effect on the constants. However for the higher viscosity data, where a true zero was used, the correction was significant. Very little effect of either flow rate or fluid (water, silicon oil or CMC solution) was found. The differences that were noted could be explained by variations in the bearing tightness due to operational temperature or use. The bearing losses measured by heat were significantly less than by torque. This is probably due to the fact that not all the heat generated in the bearings is transmitted to the operating fluid. Some is conducted away in the shaft and lost to the surroundings.

When the power data were corrected for bearing losses a normal looking power curve was obtained (Figure 10) with a $k_0 = 573.6$ in the laminar regime.

To account for restricted flow we note that Eq. 15 can be rewritten as Eq. 20.

$$\mathrm{Po} = \mathrm{Po_Z} + k_1 \frac{Q_\mathrm{M}}{\rho N D^3} \tag{20}$$

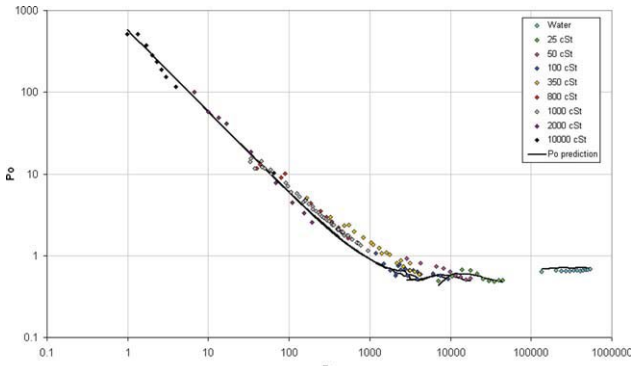

Figure 10. Power curve for Silverson 150/250 MS fitted with dual standard emulsifier rotor and stator with power numbers corrected for bearing losses.

[Color figure can be viewed in the online issue, which is available at wileyonlinelibrary.com.]

It should be noted here that, the term with k_1 is the flow number; however, we have decided to keep it in this form as the flow rate can be manually controlled so it is not a constant at a particular agitation rate. In this work we find that below a Reynolds number of around 500 that the power draw is insensitive to flow. The maximum flow the Silverson pumps decreases markedly with decreasing Re with the flow number dropping by a factor of more than 5 at Re = 1000 as illustrated by Figure 11. As Po is inversely proportional to Re in the laminar regime and the flow number decreases markedly the second term in Eq. 20 becomes insignificant and $\mathrm{Po} = \mathrm{Po_Z} = k_0/\mathrm{Re}$. In the turbulent regime $\mathrm{Po_{Z(T)}}$ is constant and it is reasonable to surmise that the transition between laminar and turbulent can be accounted for by a modification to $\mathrm{Po_Z}$ in Eq. 20. It was found that the complete curve (see fitted line in Figure 10) could be produced from Eq. 20 where $\mathrm{Po_Z}$ could be described by Eq. 21, producing Eq. 22 for the complete curve; where for the standard dual rotor-stator; $k_0 = 574$, $k_1 = 8$, and $\mathrm{Po_{Z(T)}} = 0.24$, Table 5.

$$\mathrm{Po_Z} = \frac{k_0}{\mathrm{Re}} + \mathrm{Po_{Z(T)}} \tag{21}$$

$$\mathrm{Po} = \frac{k_0}{\mathrm{Re}} + \mathrm{Po_{Z(T)}} + k_1 \frac{Q_\mathrm{M}}{\rho N D^3} \tag{22}$$

The k_0 value is much higher than for an impeller in a stirred tank. The presence of the stator is probably a big factor. Doucet et al. (2005)[3] found a high k_0 value for a batch rotor-stator device at PoRe = 314. When the stator was removed from the Silverson 150/250MS a value PoRe = 276 was found in the laminar regime. This is still higher than a stirred tank rotor due to the restrictions on flow imposed by the pumping chamber.

Metzner and Otto shear rate constant

In the case of a shear-thinning fluid obeying the power-law model, the viscosity decreases when the shear rate is

Table 5. Values of the Constants for the Silverson 150/250 MS Inline Mixer

Screens	$\mathrm{Po_{Z(T)}}$	k_1	k_0	N_Q (turbulent)	K_s
Dual standard screens	0.235	8.02	573.6	0.054	46.2
Dual fine screens	0.148	9.25	–	0.051	–
No screens	0.212	7.05	276.2	0.072	6.6

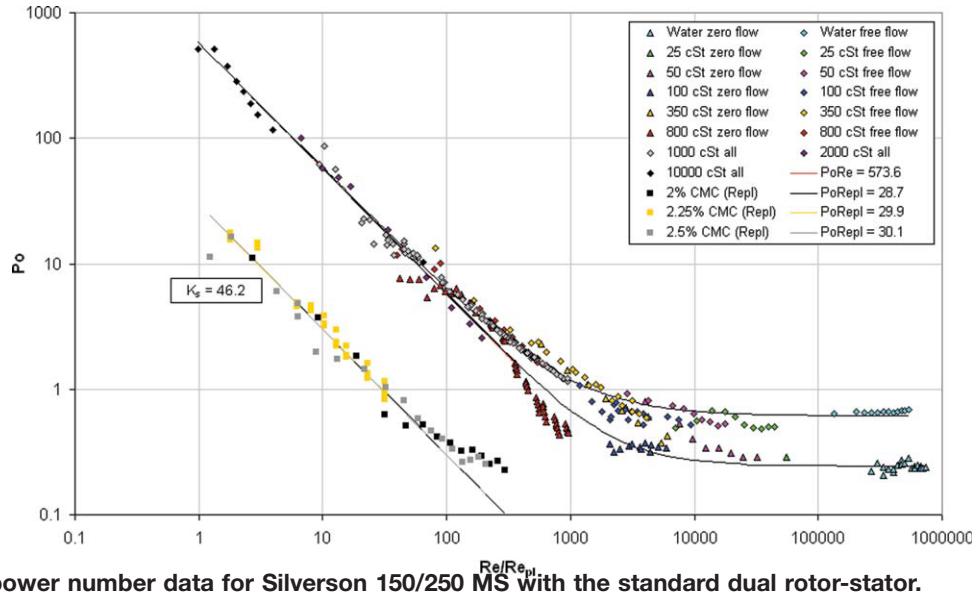

Figure 12. All power number data for Silverson 150/250 MS with the standard dual rotor-stator.

Black lines drawn to guide the eye. [Color figure can be viewed in the online issue, which is available at wileyonlinelibrary.com.]

increased. To evaluate the power consumption of such a fluid, the apparent viscosity must be determined. Metzner and Otto (1957)[5] showed that the average shear rate around the impeller can be correlated with the rotational speed by means of the proportionality parameter K_s, which is a function of the impeller geometry, Eq. 23.

$$\dot{\gamma} = K_s N \tag{23}$$

Once this parameter is known, the characteristic power curve of the agitator (Po vs. Re) using a shear-thinning fluid can be determined. The approach used to determine the K_s value was that of Rieger and Novak (1973)[11] in which a modified Reynolds number, often called the power-law Reynolds number, Re_{pl}, is used to draw the curve (Po vs. Re_{pl}); given by Eq. 24, where k and n are the consistency index and the power-law index, respectively, of the fluid.

$$\mathrm{Re}_{\mathrm{pl}} = \frac{\rho N^{2-n} D^2}{k} \tag{24}$$

In the laminar regime, the in-line Silverson mixer also has a constant value of $PoRe_{pl}$ as illustrated in Figure 12 which also shows all the power number data for all fluids and all flows plotted against Re or $Re_{pl.}$ Figure 13 shows similar data for the dual rotor with the screens removed. As the true Reynolds number of the Silverson in the laminar regime is actually given by Eq. 25, rather than Eq. 24, then a simple comparison of the laminar power constants for the non-Newtonian and the Newtonian fluids yields the Metzner-Otto constant, as in Eq. 26.

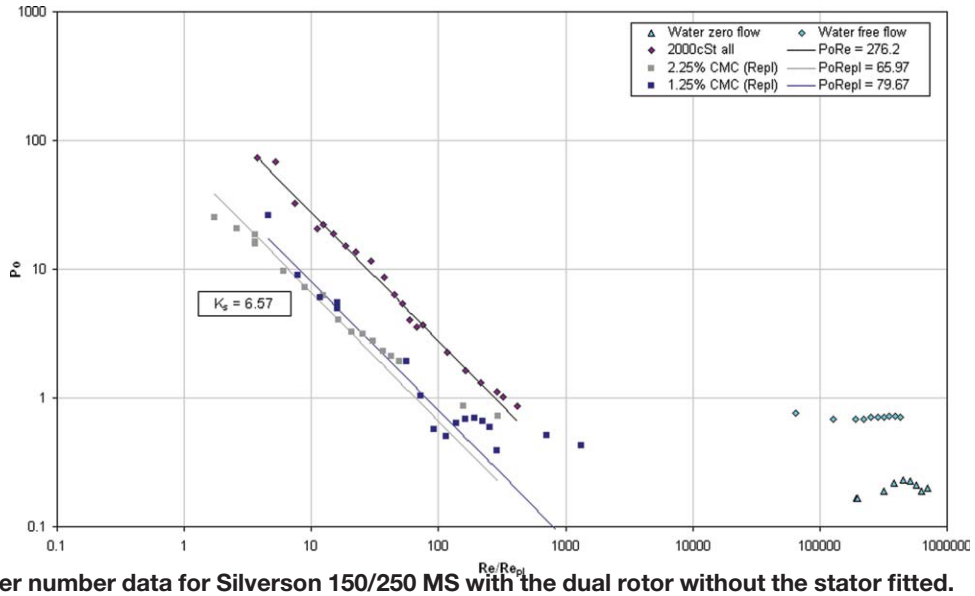

Figure 13. Power number data for Silverson 150/250 MS with the dual rotor without the stator fitted.

[Color figure can be viewed in the online issue, which is available at wileyonlinelibrary.com.]

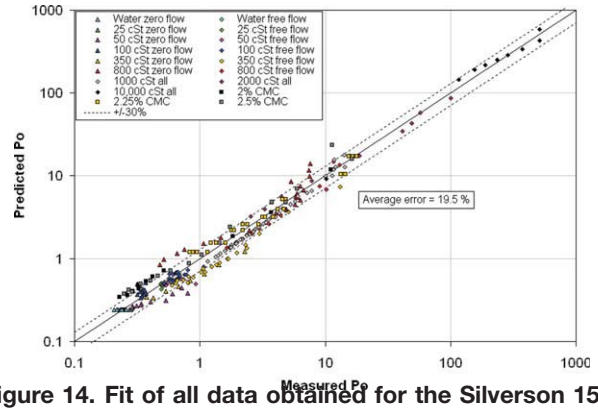

Figure 14. Fit of all data obtained for the Silverson 150/250 MS with the dual rotor and standard emulsifier screens to Eq. 22.

[Color figure can be viewed in the online issue, which is available at wileyonlinelibrary.com.]

$$\mathrm{Re} = \frac{\rho N^{2-n} D^2}{k K_s^{n-1}} \tag{25}$$

$$K_s = \left(\frac{\mathrm{PoRe_{pl}}}{\mathrm{PoRe}}\right)^{1/(n-1)} \tag{26}$$

For the dual rotor K_s values of 45.2 and 6.6 were determined for the dual standard emulsifier screen and for no screens respectively. The increase in average shear when the stator is present is a factor of 6.9. The outer stator contains seven rows of holes which seems to correlate to the increase in shear in the mixing chamber. It would be interesting to change the number of rows to see how good this correlation is.

The K_s value of 6.6 obtained without screens is around half the normally accepted value of 11.5 for a disc turbine in a stirred vessel.[12] Wu et al. (2006)[13] gives a comparison of values of K_s with flow number for a host of agitators. These show a correlation of K_s against flow number with two separate lines for radial and axial agitators. K_s decreases with decreasing flow number. These plots would predict a K_s value of around 0.5 at the flow numbers found in this work (0.05–0.07). Clearly then there is a big difference between

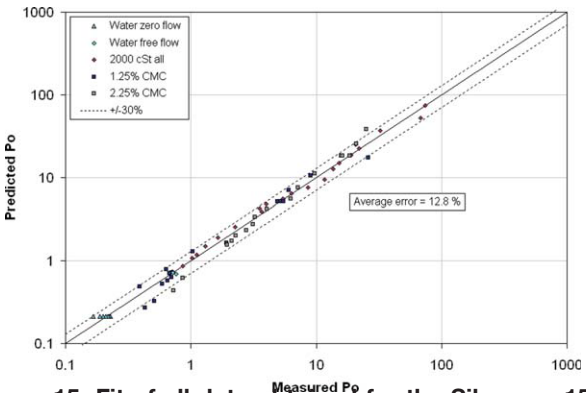

Figure 15. Fit of all data obtained for the Silverson 150/250 MS with the dual rotor and no screens to Eq. 22.

[Color figure can be viewed in the online issue, which is available at wileyonlinelibrary.com.]

average shear rates in a pumping chamber compared with a stirred tank where the clearance between the agitator tips and the walls are much greater.

The K_s value is used to calculate the apparent viscosity in the Silverson chamber and hence allows the apparent Reynolds number to be calculated. K_s value combined with Eq. 23 allows us to predict Po for all fluids (providing the viscosity law is known) and all flow rates. A comparison of the measured Po vs. the predicted values using Eq. 22 for all the data shown in Figure 12 is given in Figure 14. A similar plot for no screens is shown in Figure 15 using the constants from Table 5 and Eq. 22.

Conclusions

The constants required for the prediction of power in an in-line rotor stator mixer ($\mathrm{Po_Z}$ k_0, k_1, N_Q, and K_s) can be derived from a few relatively few simple experiments described earlier. These constants along with knowledge of the rheological properties of the fluid can be used to calculate the power number and hence power for any given flow rate and rotor speed within engineering design accuracy.

To sensibly correlate the power data for the in-line rotor-stator mixer the bearing losses power need to measured and subtracted from the total power.

At low flow rates the power draw shows an unexpected increase in the power draw which we attribute to internal recirculation around the screen holes. This can be described mathematically using pump efficiency term.[9] In most practical industrial situations this flow rate range is not important.

Acknowledgments

The authors thank David Rothman of Silverson Machines, Inc. for the provision of the high speed Silverson, Lucie Gandorf, and John Naughton who assisted with the data acquisition and processing also Craig Shore and Tony Diggle for their technical support.

Notation

Symbols

a = fitted constant, -
b = fitted constant, -
C_P = heat capacity, J kg^{-1} K^{-1}
D = outer rotor swept diameter, m
D_r = rotor diameter, m
D_s = stator screen diameter, m
d_h = stator hole diameter, m
h = characteristic length, m
K_s = Metzner-Otto shear rate constant, -
k_0 = laminar flow constant, -
k_1 = proportionality constant in the power equation, -
n_Q = flow rate constant, -
K = consistency index, -
M = torque, N m
N = rotor speed, s^{-1}
n = power law index, -
ρ = power, W
P_T = tank power term, W
P_F = flow rate power term, W
P_L = losses power term, W
Q_M = mass flow rate, kg s^{-1s}
R^2 = linear regression correlation coefficient, -
T = temperature, K

Subscripts

I = inner
O = outer
Z = zero through flow
U = free through flow

Greek letters

$\dot{\gamma}$ = average shear rate, s^{-1}
μ = dynamic viscosity, Pa s
μ_a = apparent dynamic viscosity, Pa s
ρ = density, kg m^{-3}

Dimensionless groups

Po = power number, -
Re = Reynolds number, -

Literature Cited

1. Cooke M, Naughton J, Kowalski AJ. A simple measurement method for determining the constants for the prediction of turbulent power in a Silverson MS 150/250 in-line rotor stator mixer. Presented at the Sixth International Symposium on Mixing in Industrial Process Industries, Niagara on the Lake, Niagara Falls, Ontario, Canada, August 17–21, 2008.
2. Atiemo-Obeng VA, Calabrese RV. *Rotor-stator mixing devices*. In: Paul EL, Atiemo-Obeng VA, Kresta SM, editors. *Handbook of Industrial Mixing*. Hoboken, NJ: Wiley, *Chapter 8*, 2004.
3. Doucet I, Ascanio G, Tanguy PA. Hydrodynamics characterization of rotor-stator mixer with viscous fluids. *Chem Eng Res Des*. 2005;83:1186–1195.
4. Calabrese RV, Padron GA. Power draw in radial flow batch rotor-stator mixers. Presented at the Sixth International Symposium on Mixing in Industrial Process Industries, Niagara on the Lake, Niagara Falls, Ontario, Canada, August 17–21, 2008.
5. Metzner AB, Otto RE. Agitation of non-Newtonian fluids. *AIChE J*. 1957;3:3–10.
6. Kowalski AJ. An expression for the power consumption of in-line rotor-stator devices. *Chem Eng Process*. 2009;48:581–585.
7. Sparks TG, Brown DE, Green AJ. Assessing rotor/stator mixers for rapid chemical reactions using overall power characteristics. Presented at the 1st International Conference on Process Intensification for the Chemical Industry, Antwerp, Belgium, 6–8 December, 1995.
8. Bałdyga J, Kowalski AJ, Cooke M, Jasińska M. Investigations of micromixing in the rotor-stator mixer. Presented at the XIX Polish Conference of Chemical and Process Engineering, Rzeszów, Poland, 3–7 September, 2007.
9. Cooke M, Kowalski AJ. Anomalous power draw of in-line Silverson mixers at low flow rate. Presented at the 8th World Congress of Chemical Engineering, Montreal, Canada, August 23–27, 2009.
10. Utomo TA, Baker M, Pacek AW. Flow pattern, periodicity and energy dissipation in a batch rotor-stator mixer. *Chem Eng Res Des*. 2008;86:1397–1409.
11. Rieger F, Novak V. Power consumption of agitators in highly viscous non-Newtonian liquids. *Chem Eng Res Des*. 1973;51:105–111.
12. Nienow AW. Hydrodynamics of stirred bioreactors. *Appl Mech Rev*. 1998;51:3–32.
13. Wu J, Graham LJ, Mehidi NN. Estimation of agitator flow shear rate. *AIChE J*. 2006;52:2323–2332.

Manuscript received July 23, 2010, revision received Dec. 15, 2010, and final revision received Jun. 13, 2011.